RSC Advances

REVIEW

View Article Online
View Journal | View Issue

Cite this: *RSC Adv.*, 2020, **10**, 27081

A review on tetracycline removal from aqueous systems by advanced treatment techniques

Geetha Gopal,[a] Sruthi Ann Alex,[b] N. Chandrasekaran [a] and Amitava Mukherjee *[a]

Tetracycline (TC), a frequently used drug for human and veterinary therapeutics, is among the most common antibiotic residues found in nature. Lack of advanced treatment techniques in the wastewater treatment plants (WWTPs) to remove residual TC from domestic and hospital wastewater poses a serious environmental risk. It is important to have an insight into the different advanced treatment techniques for efficient removal of TC from the surface water and in the WWTPs. The aim of this review is to discuss the nature and occurrence of TC in surface water and to present an overview of the various advanced treatment techniques for TC removal. The advanced treatment techniques include advanced oxidation processes (photolysis, ozonation, and catalytic/UV light-based degradation), membrane filtration, reverse osmosis, and adsorption techniques. Adsorption and integrated oxidation treatment techniques are the most widely studied methods, and they are widely accepted because of less cost, reusability, and toxic-free nature. Further, the uses of various types of catalysts for photodegradation and various sorbents for adsorption of TC are also presented. Finally, the importance of green nanocomposite for environmental sustainability in TC removal is emphasized.

Received 13th May 2020
Accepted 30th June 2020

DOI: 10.1039/d0ra04264a

rsc.li/rsc-advances

1. Introduction

Tetracycline (TC) is a frequently used antibiotic due to its broad-spectrum activity against bacteria (both Gram positive and negative), mycoplasma, fungus (chlamydia), rickettsiae, and parasites, and it is the primary antibiotic used for human therapy, veterinary purpose, and as a feed additive in the agricultural sector.[1] TC is the second most produced and consumed antibiotic worldwide[2] because of the following properties such as low cost, less toxicity, broad-spectrum activity, and that it can be orally administrated.[3] In addition to the human therapeutics and veterinary field, TC has been widely applied as a growth promoter in aquaculture for increasing the nutrient uptake, which in turn increases the farmer's commercial revenue.[4] TC has been frequently detected in surface and groundwater due to its extensive application and high adsorption capacity; meanwhile, the wastewater treatment plants cannot remove these micropollutants from domestic wastewater and leads to its release into the environment, which results in the presence of antibiotic residue in the ecosystem. This antibiotic residue

[a]*Centre for Nanobiotechnology, VIT, Vellore 632014, Tamil Nadu, India. E-mail: amit.mookerjea@gmail.com; amitav@vit.ac.in; Tel: +91 416 220 2620*
[b]*Centre for Nano Science and Technology, Anna University, Chennai, India*

Geetha Gopal is currently a Researcher at the Centre for Nanobiotechnology, VIT, Vellore. She has received her Master's degree in Nanoscience and Technology from AC Tech, Anna University, Chennai. She has published three research papers related to antibiotic removal in the peer-reviewed journals. Her research interest is in synthesize and characterization of nanomaterials, wastewater treatment, and nanomaterials for agricultural purposes.

Dr Sruthi Ann Alex is a Teaching Fellow in the Centre for Nanoscience and Technology (CNST), AC Tech Campus, Anna University, Chennai. She has received her Master's degree in Medical Nanotechnology from SASTRA, Thanjavur, and a doctoral degree from VIT Vellore. Her teaching and research interests include nanobiotechnology, nano sensor, and drug delivery. She has authored over 30 peer-reviewed papers in international journals and has an h-index 11 till date.

either as a parental drug or as a metabolized product or sometimes as a TC–metal complex in the environmental water matrix can cause serious environmental threats to humans as well as animals in the form of antibiotic resistance microorganism or lead to the development of a new kind of disease.[1,5]

The spread of antibiotic-resistant bacteria (ARB) in drinking water system could be facilitated by abiotic (disinfectants, chemical co-contaminants, physicochemical conditions) and biotic factors (bacterial adaptation and stress response induction).[6] The co-exposure of bacteria to heavy metals and antibiotics have led to the development of ARB and sometimes multi-antibiotic-resistant microbes. The presence of antibiotic residues will influence the structural properties of the metal ions present in the drinking water system, which can result in the deterioration of water quality.[7] Additionally, microplastics in the aquatic system can absorb organic pollutants, such as DDT, pharmaceuticals, and heavy metals, and act as a vector for these harmful pollutants in terrestrial environments,[8] which are also associated with the spreading of ARB in the marine ecosystem.[9]

The search for instant alternative techniques to remove TC from wastewater with cost-effectiveness and environmental sustainability is essential. Further, in-depth understanding of TC residues in the environmental water matrix that can result in the development of TC resistance genes and TC-resistant bacteria is very much needed. This review highlights the presence of TC in nature, its effect on the ecosystem, and the various removal methods available for TC removal from wastewater, in particular, the importance of green nanocomposites and their challenges for scale-up process.

2. TC structure, properties, and mode of action

TCs, a large group of broad-spectrum antibiotics, are of three types based on the preparation techniques such as natural, semi-synthetic, and synthetic TCs. The natural TCs such as tetracycline, oxytetracycline, and chlortetracycline were obtained by fermentation of a specific type of bacteria (*Streptomyces* sp.), while the semi-synthetically produced TCs include demeclocycline, rolitetracycline, and methacycline, and the artificially prepared TCs are doxycycline and minocycline.[10] The name 'tetracycline' was originated mainly due to its four basic ring structure. TC has three different pK_a values: pK_{a1} (protonation of oxygen bound in C_3 site), pK_{a2} (protonation of oxygen bound in C_{10} and C_{12} sites), and pK_{a3} (protonation of dimethyl functional group in C_4 site) at different pH 3.3, 7.7, and 9.7. Depending on the solution pH, TC exits in three forms, such as cationic form at pH < 3.3, zwitterionic at pH 3.3–7.7, and anionic at pH > 7.7. Thus, the increased pH will enhance the negative charge of TC; when pH reaches above 7.0, 25% of TC exists in the anionic form. The structure and species distribution of TC based on the pH are shown in Fig. 1. Furthermore, the physicochemical parameters like the solubility nature of TC were found to be 1.7 g L^{-1}, and its log K_{ow} (distribution coefficient between octanol and water) value ranges from −2.2 to −1.3, which indicates the hydrophilic nature of TC, and the K_d (solid–liquid distribution coefficient) was estimated to be 300–2000 L kg^{-1}. TC has a high solubility in alcohols (methanol, ethanol) and low solubility in organic solvents (ethyl acetate, acetone).[11] The chemical structure and speciation diagram of TC are given in Fig. 1

Dr Natarajan Chandrasekaran, Sr. Prof. & Director, Centre for Nanobiotechnology, Vellore Institute of Technology (VIT), has made several conceptually important and widely cited contributions to the area of nanobiotechnology. His areas of interest include nano emulsion and nanocomposites for wound healing gauze, cancer therapy, drug delivery systems, and study on nanoparticles–biomolecules interaction and nanoplastics in consumer products. He has 11 patents published in the area of nanobiotechnology, 278 peer-reviewed publications in Nanobiosciences (total impact of 628.659/h-index 49, total citations: >8000, i10-index 167). He has completed 21 funded projects as a PI and Co-PI. He is Fellow Royal Society for Biology (FRSB) and Fellow Royal Entomological Society of London (FRES) and Fellow Royal Society of Chemistry (FRSC).

Dr Amitava Mukherjee is Senior professor and Deputy Director of Centre for Nanobiotechnology, VIT, Vellore. His areas of interest include Green nanomaterials for sensor applications, environmental risk assessment of emerging aquatic pollutants, nano-remediation of pharmaceuticals, protein–nanoparticles interactions, and nano therapeutics. He has over 331 publications in peer-reviewed Scopus indexed journals (citation index 10 364; h-index 51; i 10-index 192). He has three granted and ten filed patents in area of materials science. He has so far received sixteen funded projects as Principal Investigator, and another nine as co-investigator from several federal agencies in India. He has been admitted as Fellow of Royal Society of Chemistry and Royal Society of Biology, UK in 2016. He currently serves as Associate Editor of Frontiers in Nanotechnology, Academic Editor in Plos One, and Member of Editorial board in Toxicology Reports, SN Applied Sciences, PNASI (Biology).

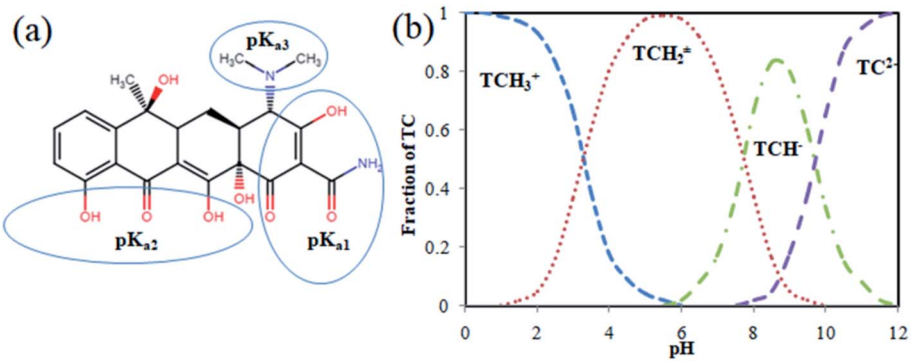

Fig. 1 (a) TC structure (b) TC speciation diagram.

3. TC occurrence and varied determinants for antibiotic resistance in the environment

The global consumption of antibiotics was 100 000–200 000 tons per year in 2002, and this number reached 34.8 billion (defined daily doses) in 2015 with a striking increase of 65% in 2000, and this was estimated to reach 4.5 trillion doses in 2020.[12] Around 2294 tons of TC was used for therapeutic purposes in the European Union during 1997, and in the USA, the TC consumption rate was increased from 3000 to 3200 tons during the period, 2000–2001. USA is the biggest consumer of TC (3200 tons per year) for veterinary medicine followed by Korea. After elimination from the human body, TC can reach the surface water due to the inability of WWTPs to remove TC effectively. The residual TC concentration in the surface water of various places around the world has been given in Table 1. The high hydrophilic and low volatile nature of TC leads to the ability of TC to persist in the environment for longer period,[1] which can facilitate the aquatic microbes to get gene mutation or gene lateral transfer for producing "antibiotic resistance genes" (ARGs),[13] and these ARGs have unfavorable properties such as persistence and ease of migration, translation, and dissemination between bacteria, and the damage caused by ARGs is more than the chronic toxicity of antibiotics alone.[14] The study on tetracycline-resistant microbes in European countries reveled the shocking truth, that is, 66.9% of *E. coli* and 44.9% of *Klebsiella* species were resistant against TC, and the global TC resistance percentage for methicillin-resistant *Staphylococcus aureus* (MRSA) and *Streptococcus pneumonia* were 8.7% and 24.3%, respectively.[15] The presence of ARB in drinking and irrigation water systems for fruits and vegetables harms human health by disturbing microflora in the human intestine, which results in the risk of infectious diseases.[16] The gastrointestinal system of humans acts as a reservoir for tetracycline resistance genes, and the presence of resistance genes *tet*(O) and *tet*(S) in bifidobacteria isolated from human gastrointestinal tract was reported.[17] Over 60 ARGs (comprising of β-lactam and TC resistance genes) were found in dairy manures in the USA, and almost all the isolated *E. coli* from these farms showed TC resistance.[18] Occurrence of four TC resistance genes, namely *tet*(O), *tet*(M), *tet*(Q), and *tet*(W), were reported in the Sumas river network of Canada in the range between 1.47×10^2 and 3.49×10^4 copies per mL.[19] The presence of ARB and ARG in aquaculture of Vietnam, Thailand, China, Korea, and India has been reported. ARG acquired bacteria have the ability to live under unfavorable conditions, and this bacteria can transform their resistance determinants to different environmental

Table 1 Reported residual TC concentration from various aqueous matrixes

Country	Aqueous matrix	Mean concentration
Portugal[12]	WWTP influents	0–32.3 ng L^{-1}
	WWTP effluents	0–22.8 ng L^{-1}
China (TGR zone)[21]	Surface water	263.60 ng L^{-1}
China (Yuen Long River)[22]	River water	2.01 ng L^{-1}
USA[23]	WWTP effluent	0.07–0.37 μg L^{-1}
	Surface water[24]	0.11 μg L^{-1}
	Ground water[24]	>0.5 μg L^{-1}
UK[10]	Surface water	Up to 0.11 μg L^{-1}
Germany[10]	Surface water	1.2–4.2 μg L^{-1}
Nigeria[25]	River water	0.1 μg L^{-1}
Zimbabwe[25]	Surface water	150 μg L^{-1}
Thailand[26]	Aquaculture water	180 ng L^{-1}
Iran[27]	Surface and ground water	5.4 to 8.1 ng L^{-1}

microorganisms and human pathogens, which can thereby cause new kinds of diseases to humans. The detection of ARGs against TC in Chinese river was investigated because of its higher production rate of aquaculture in the world, and the frequent application of TC as a feed additive. Hence, the strict regulation for using TC as a feed additive in aquaculture farms has been issued by China Agriculture Ministry.[20]

4. Various treatment techniques for TC removal from wastewater

The primary and secondary treatments of residual antibiotic wastewater in WWTP is not sufficient to remove 100% of TC; thus, the advanced and tertiary treatment of such antibiotic pollutants is much needed as the pollution increases with increased antibiotic consumption. Advanced oxidation process (AOP), such as photolysis, ozonation, Fenton, and photo-Fenton processes, and the oxidation of antibiotics in the presence of ozone/UV/hydrogen peroxide mainly involve transformation and release of oxidized products with complete removal efficiency. The vital technique to remove various kinds of pollutants is adsorption, and the main advantage of this process is the application of low-cost adsorbent with less toxicity. Adsorption and AOP are the two most widely as well as accepted techniques for the tertiary treatment of wastewater in WWTP compared to other technologies such as membrane filtration and reverse osmosis which have high production and operational cost.[12] Complete schematic diagram of TC removal by advanced treatment techniques is given in Fig. 2.

4.1. Advanced oxidation treatment techniques (AOPs)

AOPs involve the release of free radicals such as $HO^{\bullet}$, $O_2^{\bullet}$, $HO_2^{\bullet}$ and $SO_4^{\bullet}$ using various catalysts upon their interaction with ozone, hydrogen peroxide, and UV irradiation. These free radicals can influence the degradation of antibiotics into simpler byproducts and result in the complete removal of antibiotics from wastewater. TC degradation in aqueous matrices by different types of AOPs is given in Fig. 3.

4.1.1. Photolysis. It is the application of natural or simulated light source on the catalyst for the complete degradation of antibiotics, and this process is of two types: direct (the light irradiation itself will decompose the antibiotics) and indirect (light irradiation on the catalyst for the release of free radicals, which will mediate the degradation process) photolysis. Davies *et al.* reported the very first photochemical oxidation of TC in 1979, and they showed that the process mainly follows the photodeamination of TC upon interaction with molecular oxygen species.[28] This process leads to many UV-based photodegradation for TC removal. Addition of H_2O_2 during UV treatment of TC could improve the quantum yield, and the system of UV/H_2O_2 provided a decreased TOC content and reduced acute toxicity of TC degraded byproducts.[29]

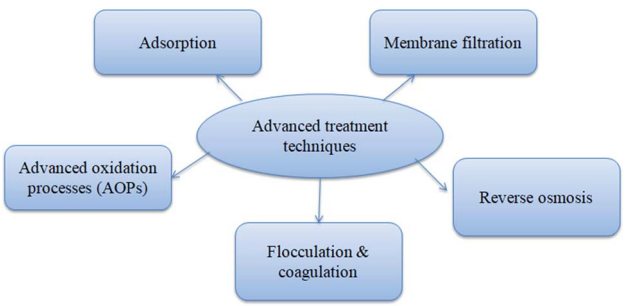

Fig. 2 Advanced treatment techniques for TC removal.

4.1.2. Heterogeneous photocatalysis. The development of heterojunction provides the direct transfer of plasmonically excited charge carriers from metal to semiconductor, and thus, reduces the recombination effect. The surface plasmon resonance (SPR) effect of metal nanoparticle occurs by passing visible light on the surface of nanoparticle and the mutual oscillation of conduction electrons on the surface of the catalyst material. Bi_2O_3 with increased active site, Ag nanoparticles with SPR effect, and montmorillonite (MMT) with high surface area were together used to form Ag-loaded Bi_2O_3/montmorillonite, and this nanocomposite can mineralize 90% of TC within 60 min of light irradiation.[30] Coupling of Bi_2O_3 with g-C_3N_4 provided efficient core–shell material with 80.2% TC removal.[31] Designing of mesoporous Ag/$Bi_2Sn_2O_7$–C_3N_4 has excellent photocatalytic effect on TC owing to its effective charge separation and SPR effect, which can influence the increased light absorption. This material can remove 89.1% of TC within 90 min.[32] Solvothermally prepared $Bi_{24}O_{31}Br_{10}$ nanosheets with controlled thickness have high charge density and charge transfer efficiency. These nanosheets can degrade 95% of TC under UV light irradiation.[33] MWCNT-coupled $Bi_4O_5Br_2$ can remove 86.2% within 120 min under UV irradiation.[34] Decoration of reduced graphene oxide (rGO) on ZnAlTi–LDH for the enhanced photocatalytic oxidation of TC of >80% under 30 W white light irradiation for 150 min.[35]

The fast recombination of e^-/h^+ pairs in TiO_2 nanosheets can be reduced by doping with Co^{2+}, and further coating of Co-doped TiO_2 on rGO sheets by one-pot hydrothermal method gives Co-TNs/rGO nanocomposite, which can remove 60% of TC within 180 min with 5-cycle repeatability.[36] The excellent chemical stability and non-toxicity of g-C_3N_4 with a moderate band-gap (2.7 eV) make it useful to synthesize a heterojunction core–shell structure consisting of Co–TiO_2 nanofibre core and g-C_3N_4 shell with the excellent photocatalytic performance for TC (90.8% removal) and disinfection activity against *E. coli*.[37] The heterojunction BiOCl/TiO_2 with flower-like morphology exhibits strong photocatalytic activity with a high surface area, which has shown 82% of TC removal within 10 min of irradiation.[38] In order to overcome aggregation and improve the reusability of TiO_2 nanoparticles, providing a coating with calcite ($CaCO_3$) is generally encouraged, and the sol–gel-synthesized CAL/TiO_2 nanocomposite shows above 90% of TC mineralization under UV irradiation.[39] A material composed of NiO–TiO_2, known as ilmenite, is formed by the coupling of $NiTiO_3$ with TiO_2 *via* co-precipitation method to provide an-heterojunction nanocomposite, and this material has the band-gap energy in the visible region and removes 58% of TC within 2 h along with efficient H_2 production.[40]

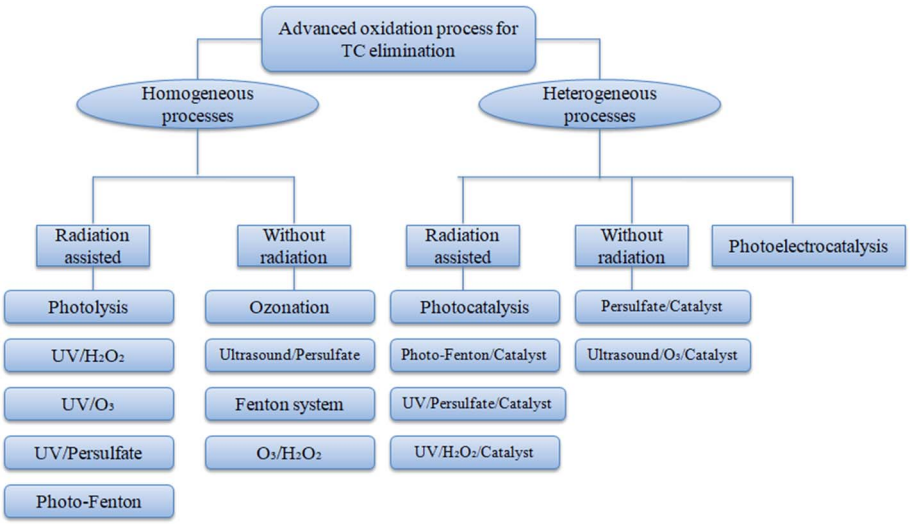

Fig. 3 Different types of AOPs for TC degradation in aqueous matrices.

Due to the wider application in pollutant removal, iron-based metal–organic frameworks (MILs) find advantages than other photocatalyst, and the report by Dongbo *et al.*(2018) proved that MILs had a combined adsorption–photocatalytic degradation effect on TC and yield 96.6% removal.[41] The magnetic $FeNi_3/SiO_2/CuS$ can degrade 96.7% of TC within 90 min,[42] while $FeNi_3@SiO_2@TiO_2$ can help in complete degradation of TC (100%) under optimized condition.[43]

Despite the narrow band gap, $BiVO_4$ semiconductors suffer deficient electron transport and ultra-low carrier mobility, which lowers their catalytic ability. Hence, doping with Bi_3TaO_7 could provide high band potential and enhanced stability for pollutant degradation. The construction of 2D–2D hetero-junction by $BiVO_4/Bi_3TaO_7$ with 0D C-dots as a bridging material helped to improve the TC degradation to 91.7% within 120 min.[44] The $BiVO_4/TiO_2$/rGO nanocomposite with excellent photocatalytic property was applied for treating four types of TCs and provided removal percentages of 96.2% (TC), 97.5% (CTC), 98.7% (OTC), and 99.6% (DXC) after 120 min of visible light irradiation. Here, rGO facilitates the electron transfer and acts as an electron reservoir for the enhancement of TC photocatalysis.[45]

The noble metal nanoparticles of Au, Ag, and Pt showed remarkable photocatalytic property in the visible light range due to its unique SPR effect. The main drawback of Ag/AgBr is the high recombination of e^-/h^+ pairs and irregular structure, which result in low catalytic activity. Pairing with a carbonaceous material can improve the charge separation as well as increase the lifetime of e^-/h^+ pairs with high photocatalytic property. The modified thermal polyol method was followed to prepare AABR–ACK (Ag/AgBr on activate carbon) composite and used to remove 92.08% of TC under visible light irradiation within 180 min.[46] The photosensitive material Ag/AgBr could be coupled with Ag_2WO_4 to improve the charge separation and visible light-harvesting capacity, and this ternary composite can remove 88.3% of TC.[47] Novel ultrasonic-assisted synthesis of rGO/Ag_2CO_3 provided better degradation efficiency compared to other rGO-based materials, and this novel material reported 91.6% removal of TC.[48] The Z-scheme AgI/WO_3 shows 75% TC degradation.[49] The narrow band gap and SPR effect of Ag/$AgIn_5S_8$ nanocomposite provides more advantages in the photocatalytic degradation of pollutants, and this material can mineralize 56.3% of TC (95.3% of TC removal) from real pharmaceutical wastes.[50] The Z-scheme photocatalytic process of 1D/2D $WO_{2.72}/ZnIn_2S_4$ hybrid nanocomposite involves faster charge separation, provides higher redox capacity, and piled-up photogenerated holes. This composite can remove 97.3% of TC by hydrothermal method.[51]

Mixed metal oxides (MMOs) exhibit better charge transfer and improved visible light absorption capacity. The fabrication of Zn/Fe-MMO was found to be useful for the enhanced photocatalytic removal of pollutants due to its layered double hydroxide structure (LDH), and this composite can remove 88% of TC under 2 h of visible light irradiation.[52] The other MMOs such as TiO_2–Fe_2O_3 has 79.75% of TC removal capacity.[53]

4.1.3. Fenton/photo-Fenton mediated. Fenton and related processes were established as effective treatment methods for the complete mineralization of different types of antibiotics. The process mainly involves the release of hydroxide radicals through the interaction between hydrogen peroxide and ferrous salt. Rossi and Nogueria reported the removal of 24 mg L^{-1} of TC *via* Fenton treatment. Further, to improve the movement of ions for better catalysis, the photo-Fenton system was introduced, which involves the application of external energy such as UV irradiation. The photo-Fenton system achieved 77% of TC mineralization with H_2O_2 as an oxygen source and UV irradiation by a mercury lamp UV TQ718.[54] The photoelectron-Fenton system comprises of Fe_3O_4–graphite cathode, which helped to reduce the dissolved O_2 to generate hydroxyl radicals for the efficient degradation of TC, and the results showed the highest degree of mineralization of about 84.3% under the optimum current density of 70 mA cm^{-2}.[55] The heterogeneous photo-

Fenton-like system, g-C_3N_4@$MnFe_2O_4$-G, with persulfate activation could remove 91.5% TC, and it has relatively high specific surface area (SSA) and fast generation of e^-/h^+pairs.[56] The novel 3D porous hydrogel made up of α-FeOOH/rGO could generate reactive oxygen species in the absence of H_2O_2 with 97.3% of TC removal that can be used as an efficient catalyst.[57]

4.1.4. Persulphate and peroxymono/disulphate mediated. Compared to hydroxyl ($^{\bullet}OH$) radicals, sulfate ($SO_4^{\bullet -}$) radicals have shown outstanding properties such as strong oxidizing power with high redox potential ($E^{\circ} = 2.5$–3.1 V, $t_{1/2} = 30$–40 μs) and stronger oxidation selectively towards organic pollutants. The most commonly used precursors for SO_4 radicals are peroxymonosulfate (PMS, HSO_5^-) and peroxydisulfate (PDS, $S_2O_8^{2-}$). Low-pressure UV (LPUV) and medium pressure UV (MPUV) are the two types of UV sources used in UV-based AOPs, in which MPUV is more effective for a large number of organic pollutants due to its wider emission spectrum with high power. The combination of MPUV/PMS system could degrade 82% of TC.[58] Degradation of TC by PDS activation under ultrasound irradiation was achieved by using 4 mM of $S_2O_8^{2-}$ with 96.5% of TC removal.[59] Natural bornite (Cu_5FeS_4) rich in Cu and Fe ions could effectively activate the PS system for TC degradation with the removal efficiency of 81.6% and mineralization percentage of 48.7%.[60] The magnetic nanocatalyst $Fe_3O_4/Na_2S_2O_8$ acts as an efficient PDS activator with ultrasound irradiation, which could remove 89% of TC within 90 min.[61] The simple and easy way to activate the PS system by thermal irradiation of 70 °C was reported with the complete elimination of TC within 30 min.[62] The highly catalytic $Ni_{0.6}Fe_{2.4}O_4$ with accelerated PS activation capacity was used to remove 86% of TC within 35 min of interaction period.[63] The ferromanganese oxides (FMOs)/PMS system could remove 94.3% of TC with increased active sites and catalytic efficiency.[64]

4.1.5. Photocatalysis with H_2 evolution. The recent advances in photocatalysis of organic pollutants with the production of H_2 paves the way for designing of photocatalytic fuel cells (PFC), which have favorable features for efficient degradation of pollutants such as usage of low-cost solar energy as light source, environmental sustainability, direct and fast release of photogenerated electrons. The usage of PFC (Fe/GTiP) with Fe, GO, and TiP (anode)/$ZnIn_2S_4$ (cathode) as an effective heterojunction composite could help in removal of 89% of TC in 90 min.[65]

4.1.6. Ozonation. Ozonation is one of the most widely used treatment techniques because of its ability to degrade complex compounds into simpler byproducts, yet it possesses difficulties due to its poor mass transfer rate and high cost. Hence, ozonation is mostly combined with other techniques such as O_3/H_2O_2, O_3/UV, O_3/ultrasound, and catalytic ozonation. The complete degradation of TC was achieved within 4–6 min by ozonation alone.[66] Ozonation of TC in an internal loop-lift reactor was performed to improve the mass transfer of ozone from gas phase to liquid phase, and the dominant ozone process gives 35% of COD removal after 90 min of ozonation.[67] The heterogeneous catalytic ozonation with accelerated mass transfer and self-cleaning efficiency of goethite catalyst against TC gives complete mineralization and reduced toxicity of byproducts against *Daphnia magna*.[68] The combination process such as O_3/activated carbon, O_3/H_2O_2, and O_3/biological treatment was followed to give completely mineralized TC with 100% degradation efficiency and toxicity-free end-products.[69] Ultrasound enhanced Fe_3O_4/O_3 system has a biochemical degradability ratio of 0.694, and the system has less energy consumption, high stability, and reusability.[70] The rectangular air-lift reactor was used for the demonstration of US-enhanced ozonation of TC, and the system gives 91% COD removal and reduced acute toxicity level from initial 95% to 60% after 90 min of reaction.[71]

4.1.7. Simultaneous TC degradation and adsorption. Mere photocatalytic treatment of TC could produce incomplete mineralization of the polyaromatic ring structure of TC, and it is not suitable for higher concentrations of pollutants. Hence, to overcome the above problem, the integration of AOPs with adsorption technology could be beneficial and provide the complete mineralization of TC from wastewater. The visible light response of Bi semiconductors due to its narrow band gap originates from the hybridization of Bi 6s and O 2p states, and the decoration of CdS nanoparticles on BiOCl provides enhanced catalytic properties like response for wider solar spectrum with efficient electron–hole separation, and the unique layered structure of BiOCl gives better adsorption of pollutants. The application of 3D BiOCl–CdS on TC under solar light irradiation for 60 min gives 91.2% removal.[72]

Different types of catalysts, along with their photocatalytic efficiencies, have been given in Table 2.

4.2. Adsorption process

Adsorption is the process of accumulation of matter either from gas or liquid to the surface of an adsorbent by physical or chemical bonding. This process finds more advantages in pollutant treatment techniques as it is simple, easy to operate, environmentally friendly, and efficient process compared to photodegradation and other membrane-based technologies.[73] The effectiveness of adsorption for antibiotic removal mainly depends on the sorbent type, and their properties include SSA, porosity, and pore diameter. The materials widely used for TC removal include carbon-based adsorbents, metal and metal oxides, metal–organic framework (MOFs), clay and minerals, mesoporous materials, polymeric resins, sludge-derived adsorbents, and biopolymer–supported metal composites (Fig. 4).[74]

4.2.1. Carbon-based materials. Carbonaceous materials such as activated carbon (AC), carbon nanotubes (CNTs), graphene oxide (GO), and biochar are widely used adsorbents for antibiotic removal due to their high adsorption capacities, large SSA, and more functional groups.[74]

4.2.2. Activated carbons. Application of activated carbons (ACs) for pollutant treatment mainly depends on surface functional groups, and the removal mechanism comprises of electrostatic interaction, ion exchange, and pollutant–sorbent functional group coordination. HNO_3 is the most frequently used chemical for surface activation of carbon to give ACs with several functional groups such as carboxylic, phenolics, lactones, and carbonyl. Surface-oxidized granular activated

Table 2 Various photocatalysts used in TC removal *via* AOPs

S. no.	Photocatalyst	Working condition	% TC removal	Reference
1	Ag/Bi_2O_3/MMT	Catalyst 1 g L^{-1}, TC 20 mg L^{-1}, 60 min, pH 3–5	90%	19
2	Bi_2O_3@g-C_3N_4	Catalyst 0.5 g L^{-1}, TC 10 mg L^{-1}, 50 min	80.2%	20
3	$Ag/Bi_2Sn_2O_7$–C_3N_4	Catalyst 1 g L^{-1}, TC 20 mg L^{-1}, dark condition 30 min, pH 6, 90 min	89.1%	21
4	Co–TNs/rGO	Catalyst 1000 mg L^{-1}, TC 30 mg L^{-1}, 180 min	60%	25
5	BiOCl–CdS composite	Catalyst 500 mg L^{-1}, TC 10 mg L^{-1}, pH 11, 60 min	91.2%	27
6	CAL/TiO_2	Catalyst 1.5 g L^{-1}, TC 50 mg L^{-1}, dark 60 min, pH 7, 300 min	90%	28
7	Fe-MIL-101	Catalyst 0.5 g L^{-1}, TC 50 mg L^{-1}, dark 60 min, pH 7, 180 min	96.6%	30
8	$FeNi_3/SiO_2$/CuS	Catalyst 0.02 g L^{-1}, TC 20 mg L^{-1}, dark condition 30 min, pH 3, 200 min	96.7%	31
9	$FeNi_3$@SiO_2@TiO_2	Catalyst 0.005 g L^{-1}, TC 10 mg L^{-1}, dark condition 30 min, pH 9, 200 min	100%	32
10	C-dots/$BiVO_4$/Bi_3TaO_7	Catalyst 500 mg L^{-1}, C-dots 3 wt%, TC 5 mg L^{-1}, pH 7, 120 min	91.7%	33
11	$BiVO_4/TiO_2$/rGO	Catalyst 250 mmol L^{-1} of $BiVO_4/TiO_2$ with 0.5% of rGO, TC 10 μg L^{-1}, dark condition 30 min, 120 min, pH 3	96.2%	34
12	AABR–ACK	Catalyst 0.3 g L^{-1}, TC 15 mg L^{-1}, 180 min	92.08%	35
13	$Ag/AgBr/Ag_2WO_4$	Catalyst 1000 mg L^{-1}, TC 20 mg L^{-1}, pH 7, dark condition 1 h, 3 h	88.3%	36
14	MPUV/PMS	PMS 0.2 mM, TC 11.25 μM, UV dose 250 mJ cm^{-2}, pH 3.7	82%	48
15	BiOCl–CdS composite	Catalyst 500 mg L^{-1}, TC 10 mg L^{-1}, pH 11, 60 min	91.2%	54

carbon (GAC_{ox}) from coconut shell waste can remove Cu and TC simultaneously with TC removal capacity of 714.8 mg g^{-1} in the presence of Cu.[75]

4.2.3. Graphene oxide (GO). The unique characteristics of GO, such as 2D structure with high surface area, more functional groups (epoxy, hydroxyl, and carboxyl groups), high chemical stability, and environmentally friendly nature, make it a potential candidate for environmental remediation, and further surface modifications could enhance the removal capacity for various organic pollutants.[76] The adsorption capacity of MGO for TC is 141.44 mg g^{-1} (ref. 77) and magnetic graphene oxide sponge (MGOS) is 473 mg g^{-1}, which is 50% higher than GO.[78] Fe_3O_4-decorated 2D/2D GO/g-C_3N_4 has TC removal capacity of 120 mg g^{-1}.[79] Magnetic GO supported with

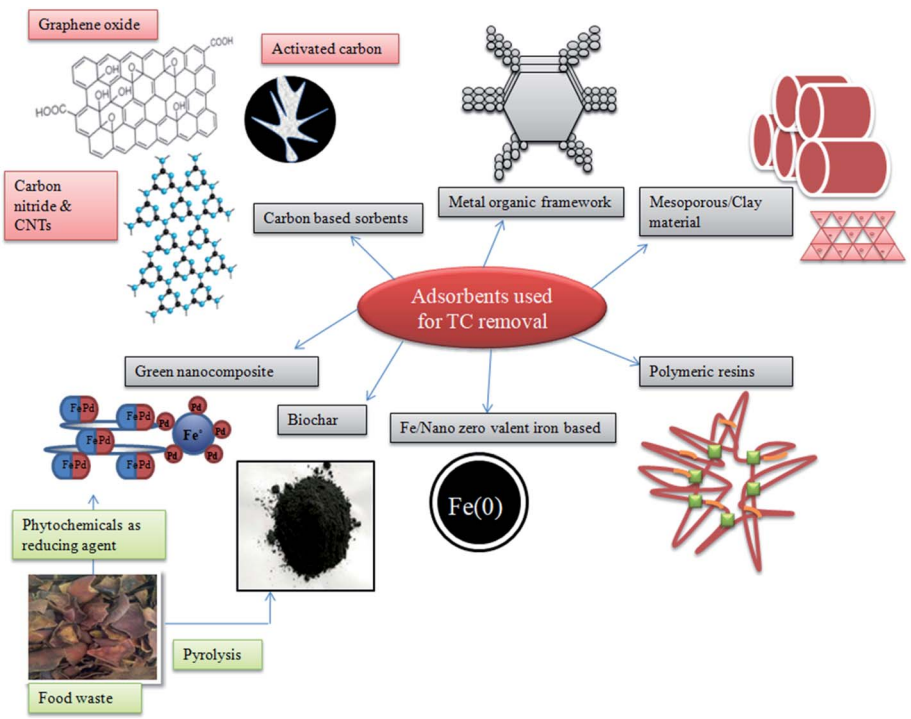

Fig. 4 Types of adsorbents for TC removal from water matrix.

diethylenetriaminepentaacetic acid (DDMGO) has more number of oxygen- and nitrogen-containing functional groups on the surface with enhanced reactivity and selectivity towards TC with removal capacity of 294.12 mg g^{-1}.[80] KOH-activated GO (G-KOH) with high SSA of 512 m^2 g^{-1} and more oxygen functional groups on the surface shows enhanced adsorption capacity for TC up to 539.59 mg g^{-1}.[81] Designing a substrate-free GO-based mircromotor finds tremendous application in antibiotic treatment. The micromotor was propelled at a high speed by the movement of oxygen in the sample, and the GO could interact with TC by π–π interaction and cation–π bonding. This synergistic effect makes it more effective and can remove 96% of TC within 30 min.[82] Fabrication of $MnFe_2O_4$/rGO by the one-pot method has an adsorption capacity of 41 mg g^{-1}.[83]

4.2.4. Carbon nitride. Among the various carbon-based materials, carbon nitrides have unique properties such as low friction coefficient, super hardness, and mechanical stability, especially graphitic carbon nitride (g-C_3N_4; g-CN) is the most frequently used metal-free polymeric material for pollutant removal. Due to its hydrophobic surface with low specific surface area and less functional groups, g-CN is often functionalized with other chemicals to get high adsorption capacity, stability, and selectivity towards pollutants in the aqueous medium. β-Cyclodextrin-modified magnetic g-CN (Fe_3O_4–g-CN@PEI–β-CD) could remove 98% of TC with a maximum adsorption capacity of 833.33 mg g^{-1}, which is much higher than other carbon-based materials.[84] Thiourea dioxides (TD) are a cheaper and safer alternative for sodium borohydride for reduction of magnetic GO (MGO), and the synthesized TDMGO can remove TC with Q_m of 1233.257 mg g^{-1} at 39.85 °C.[85] Polyimide-based CNFs, CNPs, and hydrothermally synthesized CNP nanocomposite were also used to remove TC. The results showed that the synthesized CNPs showed a higher SSA of 3561.59 m^2 g^{-1} and a larger pore volume of 4.78 cm^3 g^{-1} with a TC removal capacity of 543.48 mg g^{-1}.[86]

4.2.5. Metal–organic framework. 3D MOFs composed of metal centres/clusters and organic ligands are novel crystalline porous materials with diversified structure and tunable sizes. It can be applied to remove vast kind of pollutants, and the main attributes that improve the adsorption efficiency of 3D MOFs are its unique binding sites for better selectivity towards target pollutants, suitable particle size, and functionalized adsorption sites. UiO-67 (3D MOF) doped with 0D nitrogen/sulphur carbon dots (NSC) gives zirconium-based 3D UiO-67/NSC with TC adsorption capacity of 427.35 mg g^{-1}.[87] MWCNT/MIL-53(Fe) MOFs with a more stable and flexible structure can remove TC with Q_m of 364.37 mg g^{-1}, which is 1.24 times higher than MWCNT alone.[88]

4.2.6. Nanocomposite. Cobalt oxide–coated carbon (CoO@C) nanocomposite with less than 10 nm diameter and good magnetism property can be useful in TC remediation with a maximum adsorption capacity of 769.43 mg g^{-1}.[89] The polycondensation of chitosan and diphenylurea with formaldehyde yields pre-polymer material, and further incorporation of $MnFe_2O_4$ NPs gives magnetic polymeric nanocomposite (CDF@MF) with improved SSA of 442.6 m^2 g^{-1} and TC removal capacity of 168.42 mg g^{-1}.[90] Fabrication of Fe_3O_4@SiO_2–chitosan/GO (MSCG) nanocomposite involves the synthesis of Fe nanoparticles with silicon dioxide followed by simple precipitation with chitosan/GO solution, and the prepared MSCG have 183.47 mmol kg^{-1} TC removal capacity in the presence of Cu(II) ions.[91] Magnetic starch polyurethane polymer nanocomposite (MSPP) prepared *via* simple co-precipitation has a higher affinity for TC in aqueous solution (TC removal 19.272 mg g^{-1}) *via* cross-linking process.[92]

4.2.7. Nano zerovalent iron technology. Recently, nZVI has received much attention from scholars to work in the pollutant treatment in specific toxic pollutant remediation due to its unique attributes, specifically high surface energy, inexpensive and nontoxic nature. Due to its high surface energy, it can easily aggregate in the aqueous sample as well as the formation of the oxide layer could hinder the reactivity of nZVI. Hence, to overcome the aggregation and to improve the longevity of nZVI, doping with other metals (Ni, Cu, and Pd) could be done to form bimetallic nanoparticles in which the addition of second metal could accelerate the formation of atomic hydrogen on the nZVI surface. The bimetallic Fe/Ni nanocomposite can remove 97.4% of TC within 2 h.[93] Further, supporting the BNPs with organic matrix can improve the stability and the active sites of Fe for TC adsorption. Tabrizian *et al.* (2019) reported the Fe/Cu supported with GO shows ~100% TC removal with higher working efficacy.[94] Starch–nZVI could remove TC with a removal capacity of 4137.3 mg g^{-1} with an initial TC concentration of 100 mg L^{-1} through the flocculation process between Fe–TC complexes.[95] Novel aluminum hydroxide gel-coated NZVI (AHG@NZVI) with abundant hydroxyl functional groups could remove 98.1% of TC within 1 h, and it can be used for pretreatment of antibiotic wastewater.[96] Fe intercalated montmorillonite (Fe–Mt) with large specific surface area and pore volume has 74.4% of TC retention capacity.[97]

4.2.8. Polymeric resin. Polymer resin microspheres have several advantages that include low cost, large surface area, high porosity, and adsorption capacity. The development of polymeric resin with magnetic material could improve the effectiveness and stability of magnetic resins, which have both adsorptive and degradation ability for TC. Magnetic polystyrene EDTA microsphere resin (MPEM) could remove 90% TC upon H_2O_2 oxidation with initial TC concentration of 40 mg L^{-1}, and the removal efficiency remains till 10th cycle of reuse.[98]

4.2.9. Mesoporous/clay materials. The large surface area and ordered pore structure of mesoporous materials find application in water purification, and the regular hexagonal structure of this material are useful for the adsorption and separation of pollutants. Fabrication of A-MCM-41 through impregnation MCM-41 with zeolite A are useful for TC removal in a fixed-bed column reactor with an adsorption capacity of 419 mg g^{-1}.[99]

Hydroxyapatite, a novel environmental-friendly nanomaterial, with good biodegradability and biocompatibility along with good adsorption behavior is a potential material for pollutant removal. But the lack of dispersibility, low surface area, and lesser active sites reduce the adsorption capacity of HAP, which can be overcome by doping/impregnating with other metal ions. Fe-incorporated HAP was found to have

enhanced dispersion stability and TC adsorption capacity of 45.39 mg g^{-1}.[100]

Synthetic silicon 13× composed of silicon, oxygen, and aluminum oxides with high cation exchange capacity could influence the surface adsorption of pollutants. Fe-incorporated zeolite (Fe–zeolite) showed maximum TC adsorption capacity of 200 mg g^{-1} with 100% removal efficiency.[101] Surface activation of mesoporous zeolite–HAP by oil palm ash-derived carbon material (Z–HAP–AA) provided maximum monolayer TC adsorption capacity of 244.63 mg g^{-1} at 50 °C.[102] Synthesis of HAP composite with clay/pumice was performed to improve the separation efficiency of HAP composite after the completion of TC adsorption, and the composites HA–C and HA–P have TC adsorption capacities of 76.02 and 17.87 mg g^{-1}, respectively, with initial TC concentration of 50 mg L^{-1}.[103]

4.2.10. Biochar (BCs). The unaltered BCs obtained from *Spirulina* (SPAL-BC)[104] and *Alfalfa* (AF-BC)[105] have maximum TC adsorption capacities of 132.8 mg g^{-1} and 372.31 mg g^{-1}, respectively, compared to other BCs obtained from *Auricularia auricular* (AA-BC),[106] spent coffee grounds (SCG),[107] and rice straw (R-BC)[108] having 11.90 mg g^{-1}, 39.22 mg g^{-1}, and 14.185 mg g^{-1}, respectively. To improve the TC adsorption capacity, the surface activation of BCs was done by various external agents to provide NaOH-activated *Pinus taeda*-derived BCs (274.8 mg TC per g BC),[109] KOH-activated waste collagen fiber BC (WCF) (593.84 mg g^{-1}),[110] H_3PO-treated rice straw biochar (552 mg g^{-1}), and swine manure BC (365.4 mg g^{-1}),[111] steam-activated bamboo BC (5.029 mmol g^{-1} in the presence of Cu),[112] and acid–alkali-treated magnetic biochar (AAMS) (286.913 mg g^{-1}).[113]

Further modification with metal nanoparticles improves the pollutant removal efficiency of BCs. The improvement in TC adsorption capacity was noted for metal–BCs such as activated municipal waste sludge biochar with Fe–Cu BNPs (AWSB/Fe/Cu) composite (386.93 mg g^{-1}),[114] chitosan–Fe/S–modified biochar (BCFe–S) (150.97 mg g^{-1}), biochar–clay composite (78 mg g^{-1}),[115] spent coffee ground biochar doped with cobalt NPs (Co–SCG) (370.37 mg g^{-1}),[116] Fe/S-modified sludge-derived biochar (AWSB/Fe/S) (174.06 mg g^{-1}),[117] Fe-impregnated chicken bone-derived biochar (MCB) (98.89 mg g^{-1}),[118] metal chloride-treated *Fargesia* biochar (HT-B) (123.6 mg g^{-1}),[119] g-MoS_2-coated rice straw-derived biochar (g-MoS_2–BC) (249.45 mg g^{-1}),[120] $ZnCl_2$-treated biochar from aerobic granular sludge (Zn–BC) (93.44 mg g^{-1}).[121] The inexpensive rice husk ash (RHA) from agricultural waste could remove 83.52% of TC with an initial TC concentration of 5 mg L^{-1} and temperature of 39.85 °C.[122]

Different types of adsorbents used for TC removal and their respective TC removal percentages are given in Table 3.

4.3. Green nanomaterials/nanocomposites

With the rising concern on using nanomaterials for efficient degradation of antibiotic pollutants, "green nanomaterial"-based TC removal was found to be toxic-free, less costly, and can be considered as the best replacement for chemically synthesized nanomaterials. The polyphenols from the plant extract are responsible for the reduction of metal precursors to produce nanomaterial with controlled size, morphology, and stability through surface capping with phenol functional groups.[123] The cost-effective production of sulfonated tea waste (STW) for TC removal (381 mg g^{-1}) along with methylene blue and Cr(VI) treatment provides a very significant advancement in pollutant removal using biomass. The thermal pyrolysis of $FeCl_3$-pretreated hydrochar yields a magnetic porous carbon composite with an SSA of 349 m^2 g^{-1}.[124] Magnetite Fe_3O_4 nanoparticles, synthesized from agricultural waste, namely *V. vinifera*, *C. limon*, and *C. sativus*, can be used to remediate TC with 90% removal capacity with simultaneous removal of antibiotics such as amoxicillin, erythromycin, *etc.*[125]

Green-synthesized highly catalytic Ni/Fe BNPs are potential candidates for pollutant removal, in particular, for TC remediation; they can remove 93% of TC within 90 min of contact time. Further, this material shows improved stability of Fe and reduced residual toxicity for bacteria and algae.[126] Due to the broader application and lesser cost for production of ZnO NPs, they are useful for antibiotic sequestration; the novel ZnO-coated pistachio shell could remove TC with Q_m of 95.06.[127]

In situ bentonite-supported nZVI–Cu, synthesized using pomegranate peel extract as a reducing agent, has 95% TC removal capacity with enhanced stability and environmental sustainability.[128] Similarly, *in situ* sand-coated GS–NiFe packed in a fixed-bed column reactor was used for the continuous removal of TC from wastewater, and it was confirmed that the external mass transfer during the initial stage was the influencing factor for TC removal, and the maximum TC loading capacity of adsorbent was 978 ± 5 mg g^{-1}.[129]

Biological sludge-based adsorbent (SBA) can remove organic pollutants, and the presence of ferric groups could improve the porous structure of SBA for better adsorption of organic micropollutants. Thus, the ferric-activated SBA was developed as a cost-effective, non-toxic, and efficient TC adsorbent with Q_m of 87.87 mg g^{-1}.[130] Iron-modified bio-hydrochar (IBHC), which is an efficient green photocatalyst prepared by one-pot hydrocarbonization of sludge, has a large number of surface functional groups with dispersed ions and also acts as an efficient carbonaceous biomass material for catalyzing PS with 99.72% of TC degradation efficiency.[131] The biosorption of TC on nanocrystalline cellulose obtained from seaweed *Ulva lactuca* provided a sorption capacity of 7.73 mg g^{-1} with a desorption efficiency of 95.20% in the first cycle, which reduced to 74.4% after 3rd cycle of TC adsorption.[132]

H_3PO_4-activated carbon nanomaterial was synthesized from the hard shell of apricot stone, and the material has a high adsorption capacity of 308.33 mg of TC per g due to the improved surface properties such as high SSA of 307.6 m^2 g^{-1}, pore volume of 0.191 cm^3 g^{-1}, and pore diameter of 1.957 nm.[133] Likewise, NaOH-activated carbon from macadamia nutshell can remove TC with a high adsorption capacity of 455.33 mg g^{-1} and has a much improved SSA of 1524 m^2 g^{-1}, which is comparable with other nanocomposites; thus, this material finds potential application for TC removal.[134]

The conversion of agricultural residues (beet pulp) into sustainable activated carbon for TC removal with a good adsorption capacity of 288 mg g^{-1} with high carbon content and high SSA of

Table 3 Different sorbents for TC adsorption

S. no.	Sorbent	Process condition	Adsorption capacity	Reference
1	GAC_{ox}	Sorbent 0.4 g, TC 100 mg L^{-1}, pH 4, 25 °C, 200 h, Cu 50 mg L^{-1}	714.8 mg g^{-1}	64
2	MGO	Sorbent 66.6 mg, TC 50 mg L^{-1}, pH 4–5, 39.85 °C, 480 min	106.60 mg g^{-1}	65
3	MGOS	Sorbent 5 mg, TC 400 mg L^{-1}, pH 3.3–7.68, 34.85 °C, 48 h	473 mg g^{-1}	66
4	GO/g-C_3N_4–Fe_3O_4	Sorbent 0.03 g, TC 50 mg L^{-1}, pH 3, RT, 300 min	120 mg g^{-1}	67
5	DDMGO	Sorbent 0.09 g, TC 50 mg L^{-1}, pH 3, 39.85 °C, 24 h	294.12 mg g^{-1}	68
6	G-KOH	Sorbent 5 mg, TC 70 mg L^{-1}, pH < 7, 25 °C, 200 min	539.59 mg g^{-1}	69
7	$MnFe_2O_4$/rGO	Sorbent 5 mg, TC 10 mg L^{-1}, pH 3.3, 25 °C, 8 h	41 mg g^{-1}	71
8	Fe_3O_4–g-CN@PEI–β-CD	Sorbent 0.008 g, TC 265 mg L^{-1}, pH 9.2, 47.10 °C, 20 min	833.33 mg g^{-1}	72
9	TDMGO	Sorbent 70 g, TC 10 mg L^{-1}, pH 4, 39.85 °C, 24 h	1233.257 mg g^{-1}	73
10	UiO-67/NSC	Sorbent 20 mg, TC 80 mg L^{-1}, pH 3, RT, 120 min	427.35 mg g^{-1}	75
11	MWCNT/MIL-53(Fe)	Sorbent 0.2 g, TC 20 mg L^{-1}, pH 7, 25 °C, 1400 min	364.37 mg g^{-1}	76
12	CoO@C	Sorbent 10 mg, TC 50 mg L^{-1}, pH 8, 450 °C, 160 min	769.43 mg g^{-1}	77
13	CDF@MF	Sorbent 0.3 mg, TC 100 mg L^{-1}, pH 6, RT, 60 min	168.24 mg g^{-1}	78
14	MSCG	Sorbent 0.4 g, TC 0.1 mM, pH 6, 24.85 °C, 24 h, Cu 0.2 mM	183.47 mmol g^{-1}	79
15	MSPP	Sorbent 400 mg, TC 20 mg L^{-1}, pH 6, 25 °C, 4 h	19.272 mg g^{-1}	80
16	Fe/Ni	Sorbent 100 mg, TC 100 mg L^{-1}, pH 5, 25 °C, 2 h	97.4%	81
17	Fe/Cu–GO	Sorbent 0.25 g, TC 100 mg L^{-1}, pH 6.5, 20 °C, 15 min	201.9 mg g^{-1}	82
18	Starch–NZVI	Sorbent 0.40 g, TC 100 mg L^{-1}, pH 6, RT, 7 days	4137.3 mg g^{-1}	83
19	AHG@NZVI	Sorbent 0.1 g, TC 250 mg L^{-1}, pH 6.51, 34.85 °C, 60 min	98.1%	84
20	MPEM	Sorbent 60 mg, TC 40 mg L^{-1}, pH 6.3, 30 °C, 12 h	166 mg g^{-1}	86
21	A-MCM-41	Sorbent 0.4 g, TC 300 mg L^{-1}, pH 3, 29.85 °C, 100 min	419 mg g^{-1}	87
22	Fe–HAP	Sorbent 1 g, TC 20 mg L^{-1}, pH 5, 24.85 °C, 6 h	45.39 mg g^{-1}	88
23	Z–HAP–AA	Sorbent 1 g, TC 100 mg L^{-1}, pH 3.3, 50 °C, 600 min	244.63 mg g^{-1}	90
24	AWSB/Fe/Cu	Sorbent 0.1 g, TC 100 mg L^{-1}, pH 4, 24.85 °C, 4 h	386.93 mg g^{-1}	102

821 m^2 g^{-1} was reported.[135] Similarly, sugarcane bagasse, an agricultural waste, was transformed into a magnetic carbon nanocomposite having hierarchical pore structure, which was applied for TC adsorption (48.35 mg g^{-1}) *via* surface H-bonding and π–π interaction.[136] The synthesis of magnetic macro-reticulated cross-linked adsorbent chitosan using the biogenic waste from gastropod shells as a pore-forming agent helped to improve the porosity, which ultimately resulted in increased SSA and diffusion coefficient; the adsorption energy of TC on sorbent was calculated to be 100 kJ mol^{-1} with TC coverage of 2.51 m^2 g^{-1}.[137]

ZnO integrated with nanocellulose prepared from waste cooler straw was used as an efficient sonocatalyst; thus, the ultrasound irradiation along with PMS addition provided a degradation efficiency of 96.4% within 15 min, and the bio-toxicity test of ZnO/NC indicated the nontoxic nature of the catalyst material due to the complete conversion of TC into toxic-free byproducts.[138]

Aerobic granular sludge (ARG) treatment has several advantages, including the strong impact resistance load, high biomass, and long solid retention time, and this technique can be used for the continuous removal of pollutants with less operational cost. The removal of TC from wastewater using ARG in a sequential batch reactor (SBR) could give 90% of TC removal along with high removal efficiency of COD, NH_4^+–N, and TP.[139] The bionanocomposite alginate beads (BNC) comprises of Fe_3O_4, TiO_2, and dead biomass of TC-resistant bacteria *Acinetobacter* sp. used in a photobioreactor for the continuous TC degradation and adsorption, and the results showed 98% TC removal under UV-C irradiation.[140]

The novel heterogeneous photocatalyst, Fe@*Bacillus subtilis*, was used for the Fenton-like oxidation of TC from aqueous system with a 96% removal rate, and this system is environmentally friendly with the complete elimination of TC with negligible iron leaching.[141] Zhuang *et al.* (2019) studied the application of novel Fe_3O_4@Fe/graphene aerogel (MGA) for TC removal, and it shows higher TC and TOC removal percentage with lower iron leakage due to its fast electron transfer rate between the catalyst and the pollutant.[142] Further, they developed a double network hydrogel template FeS/graphene with improved PMS activation performance and showed a TC degradation efficiency of 0.378 L mg^{-1} min^{-1}.[143]

The adsorption capacities of various sorbents have been compared in Fig. 5.

4.4 Effect of co-pollutants on TC removal

The extensive application of heavy metals as a growth promoter in live-stock farming and commercial fertilizer and pesticides along with antibiotics leads to metal/antibiotic pollution in the environmental ecosystem. The treatment techniques for this kind of co-contaminated sites require effective and simple separation strategies; thus, the adsorption technique plays a significant role in this place.[144] Copper is one of the most commonly used salt in animal feed that is used as a growth promoter, which results in the high concentration of Cu in animal waste, and the administration of these animal wastes for soil improvement could give rise to TC–Cu contamination in the aquatic environment. The presence of Cu has as a synergistic effect on TC removal; thus, the removal percentage can be improved if TC and Cu are present together in the environmental system. The adsorption affinity of TC on chitosan was increased to 93.04 mmol kg^{-1} in the presence of 0.5 mmol L^{-1}

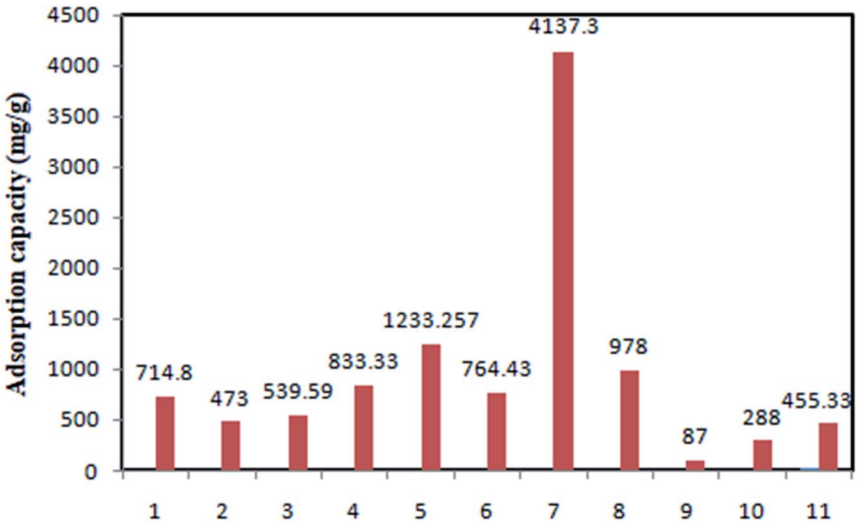

Fig. 5 Comparative evaluation of TC adsorption using different adsorbents [(1) GAC_{ox}[64] (2) MGOS[66] (3) G-KOH[69] (4) Fe_3O_4–g-CN@PEI–β-CD[72] (5) TDMGO[73] (6) CoO@C[77] (7) starch–NZVI[83] (8) GS–NiFe[124] (9) ferric-activated SBA[87] (10) AC from agricultural residual[130] (11) NaOH-activated AC from macadamia nutshell[129]].

Cu since it can act as a bridge between chitosan and TC for the enhanced adsorption rate.[145] Likewise, the effect of Cu on TC adsorption by soil and sediments was also tested. The generated water-soluble complexes, such as CuH_2L^{2+}, $CuHL^{+}$, and CuL, could be easily adsorbed with high adsorption coefficient compared to TC alone on sorbents.[146] Oxidized granular activated carbon (GAC_{ox}) was used for the simultaneous removal of TC and Cu with a maximum adsorption capacity of 714.8 mg g^{-1} for TC and 131.4 mg g^{-1} for Cu.[75] Fabrication of novel mesoporous silica adsorbent (Fe-*N*,*N*-SBA15) with a dual functional group was performed by combining di-amino functional group and Fe(III) metal ions on mesoporous silica material (SBA15), and the developed system has a high adsorption capacity of 112.3 mmol kg^{-1} with good reusability.[147] The novel ion-imprinted chitosan loaded with Fe(III) magnetic nanoparticle was used for the simultaneous removal of TC and cadmium with a maximum adsorption capacity of 516.29 mg g^{-1} for TC and 194.31 mg g^{-1} for Cd.[144] In another study, the concentration of arsenic (a critical heavy metal pollutant in the groundwater system) in groundwater was 35 times higher than the limit set by WHO. Poorly crystalline MnO_2 was used to remove both TC and As from the water matrix, and the removal efficiency depends on the concentration of As with overall TC removal percentage of around 60%.[148] Vermicomposts from biowaste can also be used as an efficient biosorbent due to its high cation exchange capacity for both organic and heavy metal pollution. He *et al.* (2017) reported the concurrent removal of heavy metals like Pb, Cd, along with TC from the mixed system with adsorption capacities of 2.99, 13.46, and 20.89 mg L^{-1}, respectively.[149] Very few studies for photocatalysis-based metal/TC removal have been reported. The Z-scheme Co_3O_4/Ag/Bi_2WO_6 was used for the simultaneous photodegradation of Cr(VI) and TC under visible light irradiation, and the system was most efficient due to the full utilization of photogenerated electrons and holes.[150]

5. Challenges faced by advance treatment techniques

AOPs release a large number of oxidized by products that could be toxic to the environment; meanwhile, the adsorption process does not release any hazardous products though it involves the adsorption of all the pollutants. However, the adsorption process requires a large amount of sorbent material that must be regenerated and disposed properly after their use. The cost of an adsorbent depends on various factors associated with the class of antibiotic to be removed. Other factors that decide the cost of sorbents are its availability, reusability, and lifetime issues. The adsorbed antibiotic should be destroyed and appropriately recovered; otherwise, it could create another type of pollutant to the environment.[12] The photocatalysis reactor consumes a large amount of energy, and the recovery of catalysts is also a tedious process.[151] Hence, the energy consumption is one of the biggest problems that result in the high cost of the process in WWTP.

The other removal techniques, such as coagulation and flocculation, have less than 20% removal capacity and release a large number of sludge products. Advanced filtration methods such as nano and ultrafiltration can remove antibiotics more effectively, but the membrane-associated problems such as fouling, high energy requirement, and high operational cost limit their application. Similarly, the reverse osmosis process for antibiotic removal has disadvantages due to its high operational cost, membrane fouling effect, and its ineffectiveness against residual antibiotic concentration.[12]

6. Conclusion and future trends

This review examines the presence of residual TC in the environmental water matrix and the advanced treatment techniques for TC remediation. Residual TC concentration in the environment has increased

tremendously due to its widespread application and the inability of WWTP to eradicate the antibiotic. Meantime, the TC–metal complex in the environment can further elevate the toxicity to a more significant extent; therefore, it is necessary to develop a removal technique that is less costly, efficient, and environmentally friendly.

From the perspective of practical design and application of the photocatalytic oxidation system, optimizing the degradation parameters is essential to ensure sustainable activity. Despite widespread investigations, it is suggested that future research should focus on photocatalyst immobilization on appropriate supporting matrices to avoid the post-separation and recovery of catalyst particles from the reaction mixture. It can be summarized that adsorption is an efficient method of eliminating TC from polluted waters with 90–100% efficacy. The high production and regeneration cost of ACs and CNTs are significant drawbacks for their usage. Hence, the word "green" plays a vital role in the development of green material-based antibiotic removal techniques with low cost and environmental sustainability. Biochars could be low-cost adsorbents, especially if they are generated as biofuel byproducts or are available as agricultural waste. Mostly, polyphenol-rich natural compounds harnessed for the synthesis of green nanoparticles have found promising use as a remedy for detoxifying toxic pollutants.

Amid many publications on TC removal, its individual and combined acute and chronic effects on the aquatic flora, fauna, and humans are not well understood. For pharmaceutically active chemicals, there have been no global permissible maximum environmental concentrations. Above all, the government should make strict regulations for all pharmaceutical industries to release zero discharge effluents. Some of the critical future research perspectives are given below:

(I) Strict laws for releasing pharmaceutical and hospital effluents should be implemented.

(II) Fabrication of sensors should be made for the continuous and accurate detection of residual antibiotic concentration in the environmental water matrix.

(III) Development of integrated adsorption–photocatalysis techniques for efficient TC removal and environmental sustainability.

(IV) Incorporating green synthesis techniques for the development of low-cost and environmentally friendly sorbents.

(V) Maximizing the removal capacity by surface modification with novel functional groups.

(VI) Improving the separation of sorbent materials after antibiotic treatment by immobilizing with a natural polymer.

(VII) The detailed study on the effect of metal ions on the removal of antibiotics and the development of a sorbent system for the efficient adsorption of metal–antibiotic complexes.

Conflicts of interest

There are no conflicts to declare.

Acknowledgements

We are thankful to the Department of Science and Technology-Science and Engineering Research Board (DST-SERB) for giving the financial support (vide sanction no. EMR/2016/004816).

References

1 R. Daghrir and P. Drogui, *Environ. Chem. Lett.*, 2013, **11**, 209–227.
2 C. Gu and K. G. Karthikeyan, *Environ. Sci. Technol.*, 2005, **39**, 2660–2667.
3 J. Jeong, W. Song, W. J. Cooper, J. Jung and J. Greaves, *Chemosphere*, 2010, **78**, 533–540.
4 F. Granados-Chinchilla and C. Rodríguez, *J. Anal. Methods Chem.*, 2017, **2017**, 1315497.
5 R. Pulicharla, K. Hegde, S. K. Brar and R. Y. Surampalli, *Environ. Pollut.*, 2017, **221**, 1–14.
6 E. Sanganyado and W. Gwenzi, *Sci. Total Environ.*, 2019, **669**, 785–797.
7 Y. Zhuang, B. Han, R. Chen and B. Shi, *Water Res.*, 2019, **165**, 114999.
8 M. Imran, K. R. Das and M. M. Naik, *Chemosphere*, 2019, **215**, 846–857.
9 B. Ram and M. Kumar, *npj Clean Water*, 2020, **3**, 1–12.
10 A. A. Borghi and M. S. A. Palma, *Braz. J. Pharm. Sci.*, 2014, **50**, 25–40.
11 P. H. Chang, Z. Li, W. T. Jiang and J. S. Jean, *Appl. Clay Sci.*, 2009, **46**, 27–36.
12 M. Patel, R. Kumar, K. Kishor, T. Mlsna, C. U. Pittman and D. Mohan, *Chem. Rev.*, 2019, **119**, 3510–3673.
13 Y. Dai, M. Liu, J. Li, S. Yang, Y. Sun, Q. Sun, W. Wang, L. Lu, K. Zhang, J. Xu, W. Zheng, Z. Hu, Y. Yang, Y. Gao and Z. Liu, *Sep. Sci. Technol.*, 2020, **55**, 1005–1021.
14 K. Kümmerer, *Chemosphere*, 2009, **75**, 417–434.
15 T. H. Grossman, *Cold Spring Harbor Perspect. Med.*, 2016, **6**, 1–24.
16 O. E. Heuer, H. Kruse, K. Grave, P. Collignon, I. Karunasagar and F. J. Angulo, *Clin. Infect. Dis.*, 2009, **49**, 1248–1253.
17 N. Wang, X. Hang, M. Zhang, X. Liu and H. Yang, *Sci. Rep.*, 2017, **7**, 1–10.
18 J. P. Oliver, C. A. Gooch, S. Lansing, J. Schueler, J. J. Hurst, L. Sassoubre, E. M. Crossette and D. S. Aga, *J. Dairy Sci.*, 2020, **103**, 1051–1071.
19 P. L. Keen, C. W. Knapp, K. J. Hall and D. W. Graham, *Sci. Total Environ.*, 2018, **628–629**, 490–498.
20 P. Gao, D. Mao, Y. Luo, L. Wang, B. Xu and L. Xu, *Water Res.*, 2012, **46**, 2355–2364.
21 L. Lu, J. Liu, Z. Li, Z. Liu, J. Guo, Y. Xiao and J. Yang, *Front. Microbiol.*, 2018, **9**, 1–12.
22 Y. Chen, K. S. Y. Leung, J. W. C. Wong and A. Selvam, *Environ. Monit. Assess.*, 2013, **185**, 745–754.
23 I. M. Al-Riyami, M. Ahmed, A. Al-Busaidi and B. S. Choudri, *Appl. Water Sci.*, 2018, **8**, 199.
24 R. I. MacKie, S. Koike, I. Krapac, J. Chee-Sanford, S. Maxwell and R. I. Aminov, *Anim. Biotechnol.*, 2006, **17**, 157–176.
25 A. C. Faleye, A. A. Adegoke, K. Ramluckan, F. Bux and T. A. Stenström, *Open Chem.*, 2018, **16**, 890–903.
26 C. S. Lundborg and A. J. Tamhankar, *BMJ*, 2017, **358**, 42–45.
27 A. Javid, A. Mesdaghinia, S. Nasseri, A. H. Mahvi, M. Alimohammadi and H. Gharibi, *J. Environ. Health Sci. Eng.*, 2016, **14**, 1–5.

28 A. K. Davies, J. F. McKellar, G. O. Phillips and A. G. Reid, *J. Chem. Soc., Perkin Trans. 2*, 1979, 369–375.
29 J. J. López-Peñalver, M. Sánchez-Polo, C. V. Gómez-Pacheco and J. Rivera-Utrilla, *J. Chem. Technol. Biotechnol.*, 2010, **85**, 1325–1333.
30 P. P. Tun, J. Wang, T. T. Khaing, X. Wu and G. Zhang, *J. Alloys Compd.*, 2020, **818**, 152836.
31 Y. Hong, C. Li, B. Yin, D. Li, Z. Zhang, B. Mao, W. Fan, W. Gu and W. Shi, *Chem. Eng. J.*, 2018, **338**, 137–146.
32 S. Heidari, M. Haghighi and M. Shabani, *Chem. Eng. J.*, 2020, **389**, 123418.
33 C. Y. Wang, X. Zhang, H. Bin Qiu, G. X. Huang and H. Q. Yu, *Appl. Catal., B*, 2017, **205**, 615–623.
34 J. Di, M. Ji, J. Xia, X. Li, W. Fan, Q. Zhang and H. Li, *J. Mol. Catal. A: Chem.*, 2016, **424**, 331–341.
35 J. Ye, J. Liu, Z. Huang, S. Wu, X. Dai, L. Zhang and L. Cui, *Chemosphere*, 2019, **227**, 505–513.
36 S. Jamali Alyani, A. Ebrahimian Pirbazari, F. Esmaeili Khalilsaraei, N. Asasian Kolur and N. Gilani, *J. Alloys Compd.*, 2019, **799**, 169–182.
37 J. Song, X. Wu, M. Zhang, C. Liu, J. Yu, G. Sun, Y. Si and B. Ding, *Chem. Eng. J.*, 2020, **379**, 122269.
38 Q. Wang, P. Li, Z. Zhang, C. Jiang, K. Zuojiao, J. Liu and Y. Wang, *J. Photochem. Photobiol., A*, 2019, **378**, 114–124.
39 N. Belhouchet, B. Hamdi, H. Chenchouni and Y. Bessekhouad, *J. Photochem. Photobiol., A*, 2019, **372**, 196–205.
40 S. K. Lakhera, H. Y. Hafeez, P. Veluswamy, V. Ganesh, A. Khan, H. Ikeda and B. Neppolian, *Appl. Surf. Sci.*, 2018, **449**, 790–798.
41 D. Wang, F. Jia, H. Wang, F. Chen, Y. Fang, W. Dong, G. Zeng, X. Li, Q. Yang and X. Yuan, *J. Colloid Interface Sci.*, 2018, **519**, 273–284.
42 N. Nasseh, L. Taghavi, B. Barikbin and M. A. Nasseri, *J. Cleaner Prod.*, 2018, **179**, 42–54.
43 M. Khodadadi, M. H. Ehrampoush, M. T. Ghaneian, A. Allahresani and A. H. Mahvi, *J. Mol. Liq.*, 2018, **255**, 224–232.
44 S. Le, W. Li, Y. Wang, X. Jiang, X. Yang and X. Wang, *J. Hazard. Mater.*, 2019, **376**, 1–11.
45 W. Wang, Q. Han, Z. Zhu, L. Zhang, S. Zhong and B. Liu, *Adv. Powder Technol.*, 2019, **30**, 1882–1896.
46 S. O. Sanni, E. L. Viljoen and A. E. Ofomaja, *J. Mol. Liq.*, 2020, **299**, 112032.
47 S. Li, W. Jiang, S. Hu, Y. Liu and J. Liu, *Mater. Lett.*, 2018, **224**, 29–32.
48 A. Reheman, K. Kadeer, K. Okitsu, M. Halidan, Y. Tursun, T. Dilinuer and A. Abulikemu, *Ultrason. Sonochem.*, 2019, **51**, 166–177.
49 T. Wang, W. Quan, D. Jiang, L. Chen, D. Li, S. Meng and M. Chen, *Chem. Eng. J.*, 2016, **300**, 280–290.
50 F. Deng, L. Zhao, X. Luo, S. Luo and D. D. Dionysiou, *Chem. Eng. J.*, 2018, **333**, 423–433.
51 W. Chen, L. Chang, S. Bin Ren, Z. C. He, G. B. Huang and X. H. Liu, *J. Hazard. Mater.*, 2020, **384**, 121308.
52 Q. Yang, S. Wang, F. Chen, K. Luo, J. Sun, C. Gong, F. Yao, X. Wang, J. Wu, X. Li, D. Wang and G. Zeng, *Catal. Commun.*, 2017, **99**, 15–19.
53 M. Galedari, M. Mehdipour Ghazi and S. Rashid Mirmasoomi, *Chem. Eng. Res. Des.*, 2019, **145**, 323–333.
54 E. Yamal-Turbay, E. Jaén, M. Graells and M. Pérez-Moya, *J. Photochem. Photobiol., A*, 2013, **267**, 11–16.
55 S. Liu, X.-r. Zhao, H.-y. Sun, R.-p. Li, Y.-f. Fang and Y.-p. Huang, *Chem. Eng. J.*, 2013, **231**, 441–448.
56 X. Wang, A. Wang and J. Ma, *J. Hazard. Mater.*, 2017, **336**, 81–92.
57 Y. Zhuang, Q. Liu, Y. Kong, C. Shen, H. Hao, D. D. Dionysiou and B. Shi, *Environ. Sci.: Nano*, 2019, **6**, 388–398.
58 X. Ao, W. Sun, S. Li, C. Yang, C. Li and Z. Lu, *Chem. Eng. J.*, 2019, **361**, 1053–1062.
59 S. Nasseri, A. H. Mahvi, M. Seyedsalehi, K. Yaghmaeian, R. Nabizadeh, M. Alimohammadi and G. H. Safari, *J. Mol. Liq.*, 2017, **241**, 704–714.
60 X. Zhang, H. Deng, G. Zhang, F. Yang and G. E. Yuan, *Chem. Eng. J.*, 2020, **381**, 122717.
61 L. Hou, H. Zhang and X. Xue, *Sep. Purif. Technol.*, 2012, **84**, 147–152.
62 Y. Ji, Y. Shi, W. Dong, X. Wen, M. Jiang and J. Lu, *Chem. Eng. J.*, 2016, **298**, 225–233.
63 R. Guan, X. Yuan, Z. Wu, H. Wang, L. Jiang, J. Zhang, Y. Li, G. Zeng and D. Mo, *Chem. Eng. J.*, 2018, **350**, 573–584.
64 Q. Yang, X. Yang, Y. Yan, C. Sun, H. Wu, J. He and D. Wang, *Chem. Eng. J.*, 2018, **348**, 263–270.
65 N. A. Nahyoon, L. Liu, K. Rabé, L. Yuan, S. A. Nahyoon and F. Yang, *Int. J. Hydrogen Energy*, 2019, **44**, 21703–21715.
66 M. H. Khan, H. Bae and J. Y. Jung, *J. Hazard. Mater.*, 2010, **181**, 659–665.
67 Y. Wang, H. Zhang, J. Zhang, C. Lu, Q. Huang, J. Wu and F. Liu, *J. Hazard. Mater.*, 2011, **192**, 35–43.
68 Y. Wang, H. Zhang and L. Chen, *Catal. Today*, 2011, **175**, 283–292.
69 C. V. Gómez-Pacheco, M. Sánchez-Polo, J. Rivera-Utrilla and J. López-Peñalver, *Chem. Eng. J.*, 2011, **178**, 115–121.
70 L. Hou, H. Zhang, L. Wang and L. Chen, *Chem. Eng. J.*, 2013, **229**, 577–584.
71 Y. Wang, H. Zhang, L. Chen, S. Wang and D. Zhang, *Sep. Purif. Technol.*, 2012, **84**, 138–146.
72 X. Bai, Y. J. Wang, Y. Li and X. J. Wang, *J. Taiwan Inst. Chem. Eng.*, 2019, **104**, 94–105.
73 Y. Xiang, Z. Xu, Y. Wei, Y. Zhou, X. Yang, Y. Yang, J. Yang, J. Zhang, L. Luo and Z. Zhou, *J. Environ. Manage.*, 2019, **237**, 128–138.
74 F. Yu, Y. Li, S. Han and J. Ma, *Chemosphere*, 2016, **153**, 365–385.
75 Q. Qin, X. Wu, L. Chen, Z. Jiang and Y. Xu, *RSC Adv.*, 2018, **8**, 1744–1752.
76 Y. Zhuang, X. Wang, L. Zhang, Z. Kou and B. Shi, *Appl. Catal., B*, 2020, **275**, 119101.
77 J. Miao, F. Wang, Y. Chen, Y. Zhu, Y. Zhou and S. Zhang, *Appl. Surf. Sci.*, 2019, **475**, 549–558.

78 B. Yu, Y. Bai, Z. Ming, H. Yang, L. Chen, X. Hu, S. Feng and S. T. Yang, *Mater. Chem. Phys.*, 2017, **198**, 283–290.
79 S. K. Sahoo, S. Padhiari, S. K. Biswal, B. B. Panda and G. Hota, *Mater. Chem. Phys.*, 2020, **244**, 122710.
80 M.-f. Li, Y.-g. Liu, S.-b. Liu, G.-m. Zeng, X.-j. Hu, X.-f. Tan, L.-h. Jiang, N. Liu, J. Wen and X.-h. Liu, *J. Colloid Interface Sci.*, 2018, **521**, 150–159.
81 J. Ma, Y. Sun and F. Yu, *R. Soc. Open Sci.*, 2017, **4**(11), 170731.
82 Y. Dong, C. Yi, S. Yang, J. Wang, P. Chen, X. Liu, W. Du, S. Wang and B. F. Liu, *Nanoscale*, 2019, **11**, 4562–4570.
83 J. Bao, Y. Zhu, S. Yuan, F. Wang, H. Tang, Z. Bao, H. Zhou and Y. Chen, *Nanoscale Res. Lett.*, 2018, **13**, 396.
84 M. Foroughi, M. H. Ahmadi Azqhandi and S. Kakhki, *J. Hazard. Mater.*, 2020, **388**, 121769.
85 Y. Yang, X. Hu, Y. Zhao, L. Cui, Z. Huang, J. Long, J. Xu, J. Deng, C. Wu and W. Liao, *J. Colloid Interface Sci.*, 2017, **495**, 68–77.
86 S. Li, Y. Zhang, Q. You, Q. Wang, G. Liao and D. Wang, *Colloids Surf., A*, 2018, **558**, 392–401.
87 Q. Yang, H. Hong and Y. Luo, *Chem. Eng. J.*, 2019, 123680.
88 W. Xiong, G. Zeng, Z. Yang, Y. Zhou, C. Zhang, M. Cheng, Y. Liu, L. Hu, J. Wan, C. Zhou, R. Xu and X. Li, *Sci. Total Environ.*, 2018, **627**, 235–244.
89 G. Yang, Q. Gao, S. Yang, S. Yin, X. Cai, X. Yu, S. Zhang and Y. Fang, *Chemosphere*, 2020, **239**, 124831.
90 T. Ahamad, Ruksana, A. A. Chaudhary, M. Naushad and S. M. Alshehri, *Int. J. Biol. Macromol.*, 2019, **134**, 180–188.
91 B. Huang, Y. Liu, B. Li, S. Liu, G. Zeng, Z. Zeng, X. Wang, Q. Ning, B. Zheng and C. Yang, *Carbohydr. Polym.*, 2017, **157**, 576–585.
92 C. P. Okoli and A. E. Ofomaja, *J. Cleaner Prod.*, 2019, **217**, 42–55.
93 H. Dong, Z. Jiang, C. Zhang, J. Deng, K. Hou, Y. Cheng, L. Zhang and G. Zeng, *J. Colloid Interface Sci.*, 2018, **513**, 117–125.
94 P. Tabrizian, W. Ma, A. Bakr and M. S. Rahaman, *J. Colloid Interface Sci.*, 2019, **534**, 549–562.
95 Y. Fu, L. Peng, Q. Zeng, Y. Yang, H. Song, J. Shao, S. Liu and J. Gu, *Chem. Eng. J.*, 2015, **270**, 631–640.
96 X. Wang, B. Zhang, J. Ma and P. Ning, *J. Environ. Sci.*, 2020, **89**, 194–205.
97 H. Wu, H. Xie, G. He, Y. Guan and Y. Zhang, *Appl. Clay Sci.*, 2016, **119**, 161–169.
98 B. Li, J. Ma, L. Zhou and Y. Qiu, *Chem. Eng. J.*, 2017, **330**, 191–201.
99 M. Liu, L.-a. Hou, S. Yu, B. Xi, Y. Zhao and X. Xia, *Chem. Eng. J.*, 2013, **223**, 678–687.
100 Y. Li, S. Wang, Y. Zhang, R. Han and W. Wei, *J. Mol. Liq.*, 2017, **247**, 171–181.
101 M. H. Jannat Abadi, S. M. M. Nouri, R. Zhiani, H. D. Heydarzadeh and A. Motavalizadehkakhky, *Int. J. Ind. Chem.*, 2019, **10**, 291–300.
102 W. A. Khanday and B. H. Hameed, *Fuel*, 2018, **215**, 499–505.
103 M. Ersan, U. A. Guler, U. Acikel and M. Sarioglu, *Process Saf. Environ. Prot.*, 2015, **96**, 22–32.
104 Y. K. Choi, T. R. Choi, R. Gurav, S. K. Bhatia, Y. L. Park, H. J. Kim, E. Kan and Y. H. Yang, *Sci. Total Environ.*, 2020, **710**, 136282.
105 H. M. Jang and E. Kan, *Bioresour. Technol.*, 2019, **274**, 162–172.
106 Y. Dai, J. Li and D. Shan, *Chemosphere*, 2020, **238**, 124432.
107 V. T. Nguyen, T. B. Nguyen, C. W. Chen, C. M. Hung, T. D. H. Vo, J. H. Chang and C. Di Dong, *Bioresour. Technol.*, 2019, **284**, 197–203.
108 H. Wang, C. Fang, Q. Wang, Y. Chu, Y. Song, Y. Chen and X. Xue, *RSC Adv.*, 2018, **8**, 16260–16268.
109 H. M. Jang, S. Yoo, Y. K. Choi, S. Park and E. Kan, *Bioresour. Technol.*, 2018, **259**, 24–31.
110 X. Wei, R. Zhang, W. Zhang, Y. Yuan and B. Lai, *RSC Adv.*, 2019, **9**, 39355–39366.
111 T. Chen, L. Luo, S. Deng, G. Shi, S. Zhang, Y. Zhang, O. Deng, L. Wang, J. Zhang and L. Wei, *Bioresour. Technol.*, 2018, **267**, 431–437.
112 R. Z. Wang, D. L. Huang, Y. G. Liu, C. Zhang, C. Lai, X. Wang, G. M. Zeng, Q. Zhang, X. M. Gong and P. Xu, *J. Hazard. Mater.*, 2020, **384**, 121470.
113 L. Tang, J. Yu, Y. Pang, G. Zeng, Y. Deng, J. Wang, X. Ren, S. Ye, B. Peng and H. Feng, *Chem. Eng. J.*, 2018, **336**, 160–169.
114 J. Ma, B. Zhou, H. Zhang, W. Zhang and Z. Wang, *Chem. Eng. Res. Des.*, 2019, **149**, 209–219.
115 K. S. D. Premarathna, A. U. Rajapaksha, N. Adassoriya, B. Sarkar, N. M. S. Sirimuthu, A. Cooray, Y. S. Ok and M. Vithanage, *J. Environ. Manage.*, 2019, **238**, 315–322.
116 V. T. Nguyen, T. B. Nguyen, C. W. Chen, C. M. Hung, C. P. Huang and C. Di Dong, *Bioresour. Technol.*, 2019, **292**, 121954.
117 J. Ma, B. Zhou, H. Zhang and W. Zhang, *Powder Technol.*, 2020, **364**, 889–900.
118 A. A. Oladipo and A. O. Ifebajo, *J. Environ. Manage.*, 2018, **209**, 9–16.
119 C. Ma, H. Huang, X. Gao, T. Wang, Z. Zhu, P. Huo, Y. Liu and Y. Yan, *J. Taiwan Inst. Chem. Eng.*, 2018, **91**, 299–308.
120 Z. Zeng, S. Ye, H. Wu, R. Xiao, G. Zeng, J. Liang, C. Zhang, J. Yu, Y. Fang and B. Song, *Sci. Total Environ.*, 2019, **648**, 206–217.
121 L. Yan, Y. Liu, Y. Zhang, S. Liu, C. Wang, W. Chen, C. Liu, Z. Chen and Y. Zhang, *Bioresour. Technol.*, 2020, **297**, 122381.
122 Y. Chen, F. Wang, L. Duan, H. Yang and J. Gao, *J. Mol. Liq.*, 2016, **222**, 487–494.
123 S. Kuppusamy, P. Thavamani, M. Megharaj and R. Naidu, *Environ. Technol. Innov.*, 2015, **4**, 17–28.
124 X. Zhu, Y. Liu, F. Qian, C. Zhou, S. Zhang and J. Chen, *Bioresour. Technol.*, 2014, **154**, 209–214.
125 M. Stan, I. Lung, M. L. Soran, C. Leostean, A. Popa, M. Stefan, M. D. Lazar, O. Opris, T. D. Silipas and A. S. Porav, *Process Saf. Environ. Prot.*, 2017, **107**, 357–372.
126 K. V. G. Ravikumar, S. V. Sudakaran, K. Ravichandran, M. Pulimi, C. Natarajan and A. Mukherjee, *J. Cleaner Prod.*, 2019, **210**, 767–776.

127 A. A. Mohammed and S. L. Kareem, *Alexandria Eng. J.*, 2019, **58**, 917–928.
128 G. Gopal, H. Sankar, C. Natarajan and A. Mukherjee, *J. Environ. Manage.*, 2020, **254**, 109812.
129 K. V. G. Ravikumar, G. Debayan, P. Mrudula, N. Chandrasekaran and A. Mukherjee, *Front. Environ. Sci. Eng.*, 2020, **14**, 1–13.
130 X. Yang, G. Xu, H. Yu and Z. Zhang, *Bioresour. Technol.*, 2016, **211**, 566–573.
131 J. Wei, Y. Liu, Y. Zhu and J. Li, *Chemosphere*, 2020, **247**, 125854.
132 M. Rathod, S. Haldar and S. Basha, *Ecol. Eng.*, 2015, **84**, 240–249.
133 M. H. Marzbali, M. Esmaieli, H. Abolghasemi and M. H. Marzbali, *Process Saf. Environ. Prot.*, 2016, **102**, 700–709.
134 A. C. Martins, O. Pezoti, A. L. Cazetta, K. C. Bedin, D. A. S. Yamazaki, G. F. G. Bandoch, T. Asefa, J. V. Visentainer and V. C. Almeida, *Chem. Eng. J.*, 2015, **260**, 291–299.
135 J. Torres-Pérez, C. Gérente and Y. Andrès, *Chin. J. Chem. Eng.*, 2012, **20**, 524–529.
136 N. Rattanachueskul, A. Saning, S. Kaowphong, N. Chumha and L. Chuenchom, *Bioresour. Technol.*, 2017, **226**, 164–172.
137 N. A. Oladoja, R. O. A. Adelagun, A. L. Ahmad, E. I. Unuabonah and H. A. Bello, *Colloids Surf., B*, 2014, **117**, 51–59.
138 R. D. C. Soltani, M. Mashayekhi, M. Naderi, G. Boczkaj, S. Jorfi and M. Safari, *Ultrason. Sonochem.*, 2019, **55**, 117–124.
139 X. Wang, Z. Chen, J. Kang, X. Zhao and J. Shen, *RSC Adv.*, 2018, **8**, 18284–18293.
140 G. Gopal, N. Roy, N. Chandrasekaran and A. Mukherjee, *ACS Omega*, 2019, **4**, 17504–17510.
141 P. Zheng, B. Bai, W. Guan, H. Wang and Y. Suo, *RSC Adv.*, 2016, **6**, 4101–4107.
142 Y. Zhuang, X. Wang, L. Zhang, D. D. Dionysiou and B. Shi, *Environ. Sci.: Nano*, 2019, **6**, 3232–3241.
143 Y. Zhuang, X. Wang, L. Zhang, D. D. Dionysiou, Z. Kou and B. Shi, *Environ. Sci.: Nano*, 2020, **7**, 817–828.
144 A. Chen, C. Shang, J. Shao, Y. Lin, S. Luo, J. Zhang, H. Huang, M. Lei and Q. Zeng, *Carbohydr. Polym.*, 2017, **155**, 19–27.
145 J. Kang, H. Liu, Y.-M. Zheng, J. Qu and J. P. Chen, *J. Colloid Interface Sci.*, 2010, **344**, 117–125.
146 Z. Zhang, K. Sun, B. Gao, G. Zhang, X. Liu and Y. Zhao, *J. Hazard. Mater.*, 2011, **190**, 856–862.
147 Z. Zhang, H. Liu, L. Wu, H. Lan and J. Qu, *Chemosphere*, 2015, **138**, 625–632.
148 H. Wang, D. Zhang, S. Mou, W. Song, F. A. Al-Misned, M. G. Mortuza and X. Pan, *Chemosphere*, 2015, **136**, 102–110.
149 X. He, Y. Zhang, M. Shen, Y. Tian, K. Zheng and G. Zeng, *Environ. Sci. Pollut. Res.*, 2017, **24**, 8375–8384.
150 J. Wan, P. Xue, R. Wang, L. Liu, E. Liu, X. Bai, J. Fan and X. Hu, *Appl. Surf. Sci.*, 2019, **483**, 677–687.
151 F. Saadati, N. Keramati and M. M. Ghazi, *Crit. Rev. Environ. Sci. Technol.*, 2016, **46**, 757–782.